

Electronic supplementary information

Electrochemical Synthesis of Polyaniline Cross-linked NiMoO₄ Nanofibre Dendrites for Energy Storage Devices

Ramya Ramkumar and Manickam Minakshi Sundaram*

School of Engineering and Information Technology, Murdoch University, WA 6150, Australia

I. Physical characterization of as-prepared NiMoO₄ powder

The as-prepared nickel molybdate (NiMoO₄) powder was characterized by X-ray diffraction (XRD) using Siemens D500 X-ray diffractometer 5635 with Cu K α radiation in the 2 θ range from 10 to 60° using a scanning rate of 1°/min. Infra-red (IR) spectroscopy was performed in the mid IR region from 550 to 1100 cm⁻¹, using a via FT-IR spectrometer (Bruker) in transmittance mode. The morphology of the as-prepared NiMoO₄ powder synthesized at 300° C was investigated using high magnification Zeiss Neon 40EsB focussed ion beam-scanning electron microscope (FIB-SEM).

A pure monoclinic NiMoO₄ (α - phase) was synthesized at a low temperature of 300 °C through combustion synthesis without any further calcination. This is possible due to the heat energy liberated by the exothermic reactions using urea as a fuel. All the diffraction peaks in Fig. S1 can be indexed as NiMoO₄ (JCPDS card no. 86-0361).¹ A quite well defined diffraction peaks reflect the characteristics of solids structurally ordered in a monoclinic crystal structure. The obtained XRD pattern is quite similar to the work reported for this material in the literature.¹⁻³

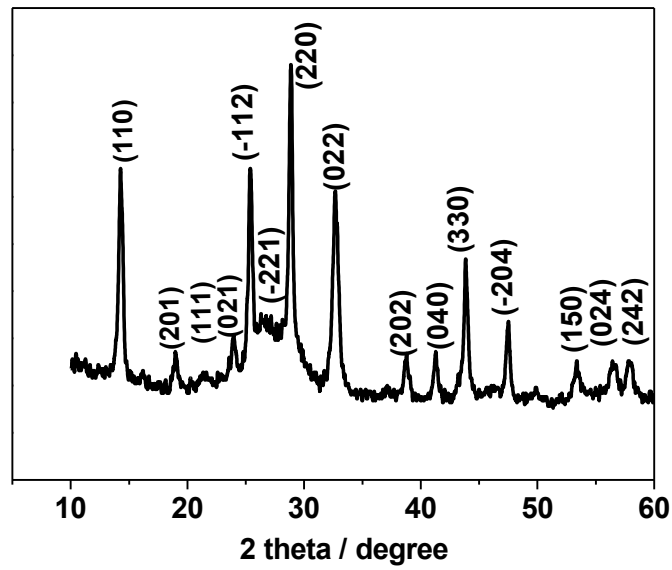


Figure S1 X-ray diffraction pattern of as-prepared NiMoO₄ powder.

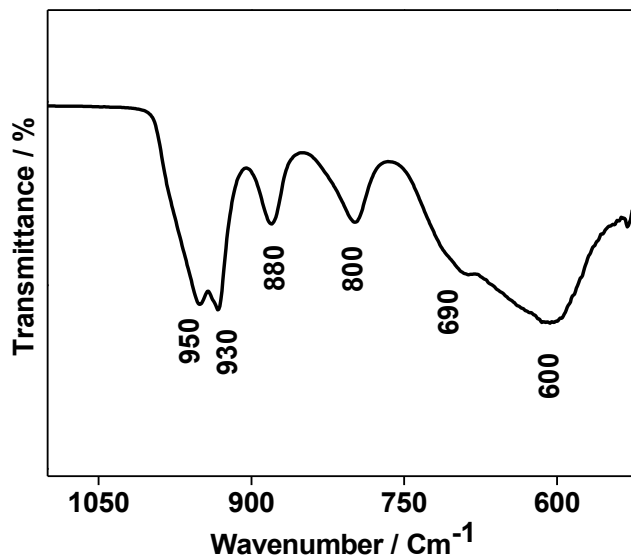


Figure S2 Infra-red spectra of as-prepared NiMoO₄ powder.

To study the bonding nature of the as-prepared nickel molybdate, infra-red spectra was performed on the powder sample and the corresponding spectrum is shown in Fig. S2. The infra-red spectrum shows peaks at 950, 930, 880, 800, 690 and 600 cm⁻¹ implying the

characteristic absorption peaks of α -NiMoO₄ structure. The bands obtained at higher and lower wavenumbers can be attributed to the vibrational modes of Mo – O – Mo and Ni – O – Mo respectively in the building block of NiMoO₄ material. ⁴ To be more specific, doublet in the 900 cm⁻¹ region corresponds to MoO₆ being in octahedral cluster while the bands observed in the 800 cm⁻¹ region corresponds to stretching vibrations of Mo – O – Mo. The broad absorption region observed in the 600 cm⁻¹ region is the superposition of Mo – O and NiO₆ building blocks of NiMoO₄. ⁵⁻⁶ The microscopic images and the elemental analysis of as-prepared NiMoO₄ under different magnifications are shown in Fig. S3.

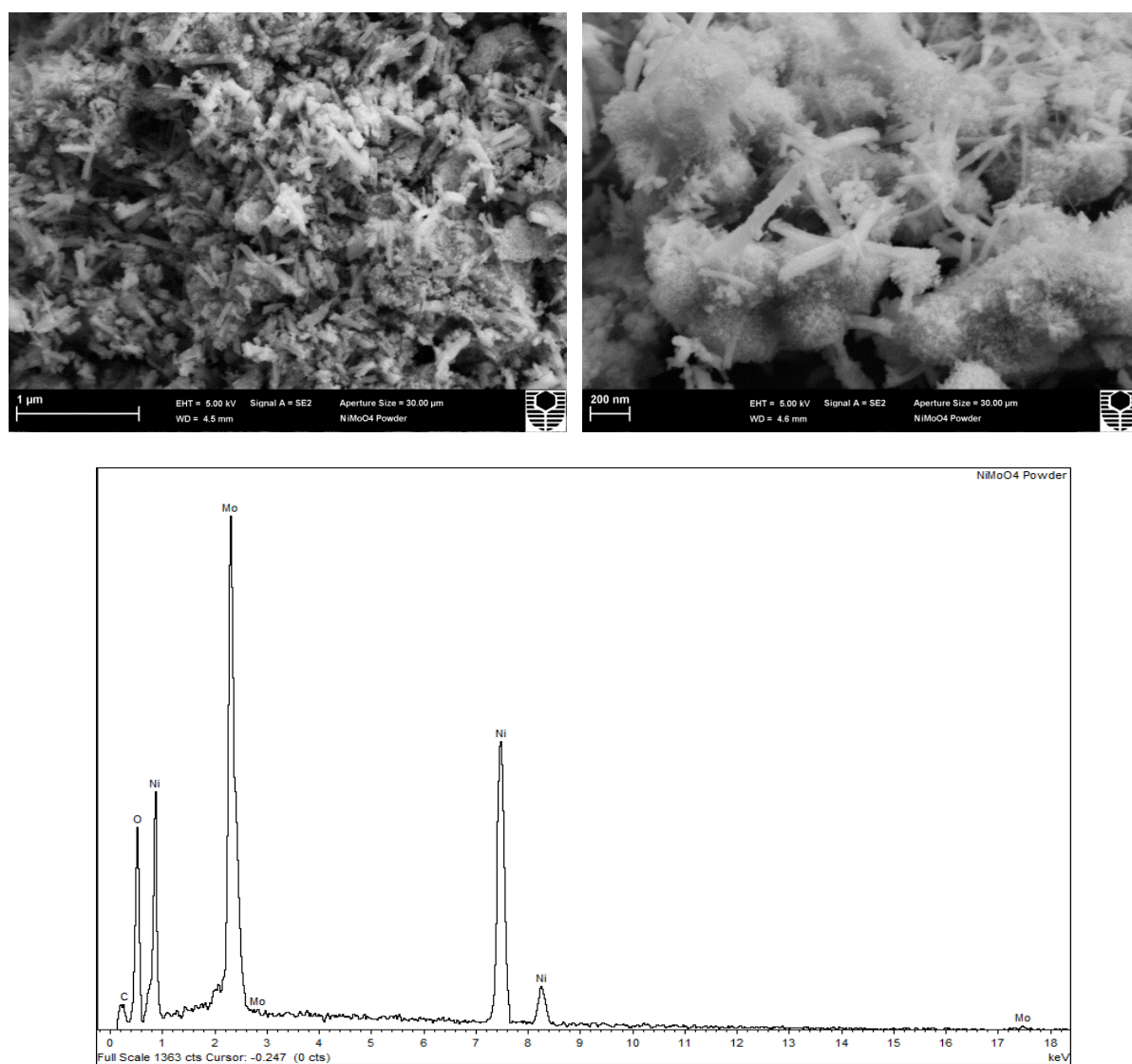


Figure S3 FIB-SEM images on different magnifications and its corresponding EDS spectra of as-prepared NiMoO₄ powder.

The NiMoO₄ powders exhibit nanorods in shape with a length of 200 – 300 nm having a diameter of 10 – 20 nm. The nanorod shaped particles were lying on poly dispersed particles with a particle size of 300 – 400 nm are porous in nature. The corresponding elemental dispersive analysis of the nanorod shaped particles indicates the presence of Ni, Mo, and O confirming the as-prepared material is nickel molybdate.

Figure S4 shows the nitrogen-sorption isotherm and Barrett-Joyner-Halenda (BJH) pore diameter distributions (in the inset) for the NiMoO₄ material exhibiting the surface area of 35.78 m²/g. The shape of the hysteresis loop implies type II behaviour in which the adsorption and desorption curves are nearly identical, having particles of partly in porous nature. The BJH pore diameter and pore volume confirmed that the as-prepared NiMoO₄ are not highly porous and hence the low surface area.

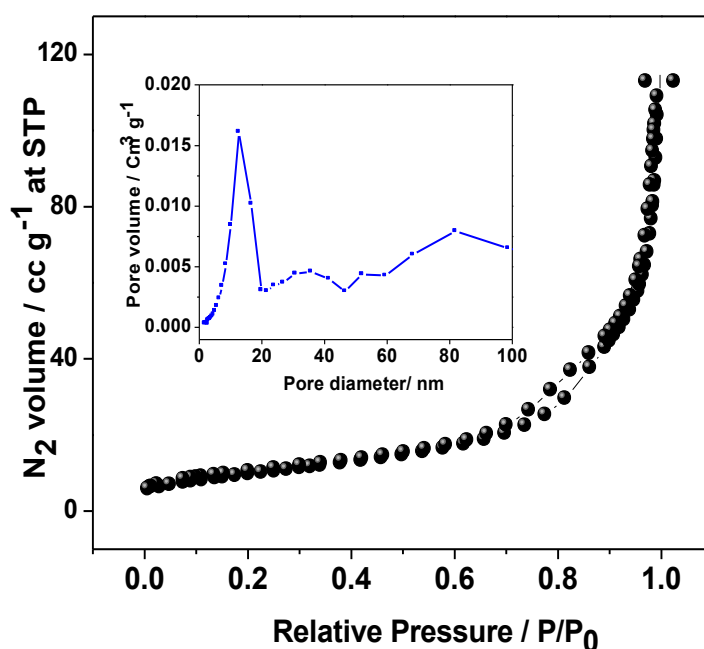


Figure S4 Nitrogen-sorption isotherm for as-prepared NiMoO₄ powder. BJH pore size distribution is shown in the inset.

II. Electrochemical deposition of as-prepared NiMoO₄ powder in PANI matrix

Incorporation of nickel ions in PANI matrix under similar deposition conditions but varying the amount of NiMoO₄ in the bath has been investigated and optimised for further experiments. As the nickel concentration in the PANI matrix is considered an important factor in redox activity, the electrolytic bath concentration plays a role in the electrodeposition of PANI/NiMoO₄ composites. The electrochemical synthesis of PANI/NiMoO₄ was prepared using nickel molybdate concentration varying from 2.5 to 15 mg in the 1 M PTSA electrolyte containing 0.1 M monomer aniline. The obtained composites were tested for capacitor applications and the electrochemical performance is plotted in Fig. S5. With increasing the NiMoO₄ content in bath from 2.5 mg, the specific capacitance increased from 320 mF cm⁻² to a maximum value of 685 mF cm⁻² initially, and then kept constant at this value. When the concentration is too low, insufficient amount of Ni²⁺ ions resulted in a lower capacitance. However, when the concentration is too high (over 10 mg), the observed plateau in capacitance indicates the metal ion adsorption into PANI matrix is diffusion limited.

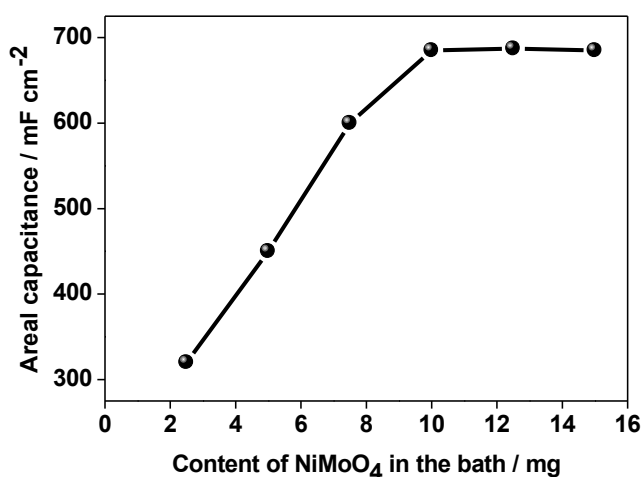


Figure S5 Variation of nickel molybdate (NiMoO₄) content in the electrolytic bath and its influence in capacitance.

III. Physical characterization of PANI/cross-linked NiMoO₄

The surface morphology and the nanostructure of PANI/cross-linked NiMoO₄ were evidenced from transmission electron microscopy. Figure S6a shows the polymerized sample is nanoparticulates, revealing dendrite like structure ranging from 200 – 400 nm. The selected area diffraction pattern (Fig. S6b) is from a single dendrite particle showing diffraction spots evidencing the crystalline nature of PANI/cross-linked NiMoO₄. Figure S6c also shows a spongy porous region with nanofibers giving more access to ions from the electrolyte and thus enhancing the electrochemical behaviour. The energy dispersive analysis (in Fig. S6d) confirmed all phases were free from any impurities and contained only Ni, Mo, C and O. The peaks corresponding to Cu are from the sample holder. Interestingly, peaks corresponding to carbon are found to be higher in intensity for cross-linked samples than that for the pure NiMoO₄ (Fig. S3). The observed difference in carbon content could be attributed to a biopolymer chitosan which is in agreement with the XPS results obtained for C 1s spectra in Fig. 9.

The as-prepared NiMoO₄ has been studied using cyclic voltammetry in a three-electrode configuration in 1 M Na₂SO₄ as the electrode. Figure S7 (A) shows the typical cyclic voltammetric (CV) curves exhibiting a pair of strong redox peaks (C₁ and A₁) indicating faradaic reactions involving Ni²⁺/Ni³⁺ couple.¹ The shape of the (CV) curves remains unchanged after multiple cycles showing the NiMoO₄ is electrochemically reversible. In accordance with the objectives of this work, the effect of composites was determined by carrying out CV on the PANI matrix in the absence and presence of NiMoO₄ with biopolymer under identical conditions. The CV profiles of these composites are compared in Fig. S7 (B). Evidently, the PANI/cross-linked NiMoO₄ showed a higher current response which is two orders of magnitude than the pure NiMoO₄. Although the current response for PANI/NiMoO₄ is higher than the pure NiMoO₄ but it is still inferior to the cross-

linked matrix. This shows the presence of chitosan moiety adheres to the host molybdate and enhances the redox reactions while improving the capacitance of the NiMoO₄ material.

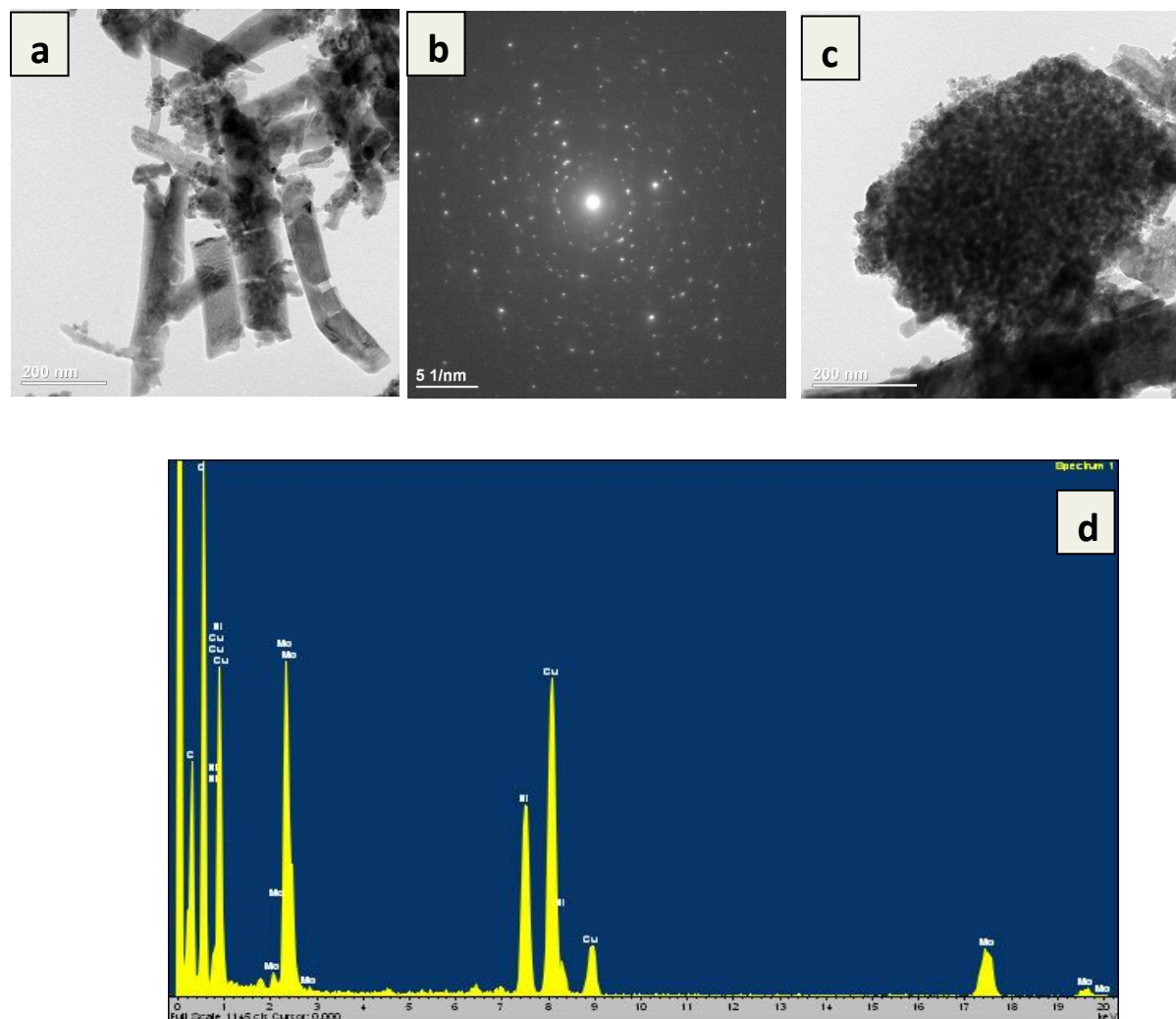


Figure S6 TEM imaging of PANI/ cross-linked NiMoO₄ (a) showing nanoparticulates, (b) its corresponding selected area diffraction pattern, (c) region showing a nanofibrous like particles and (d) a representative EDS spectrum illustrating C, Ni, Mo, O and C peaks. The Cu peak is from the sample holder.

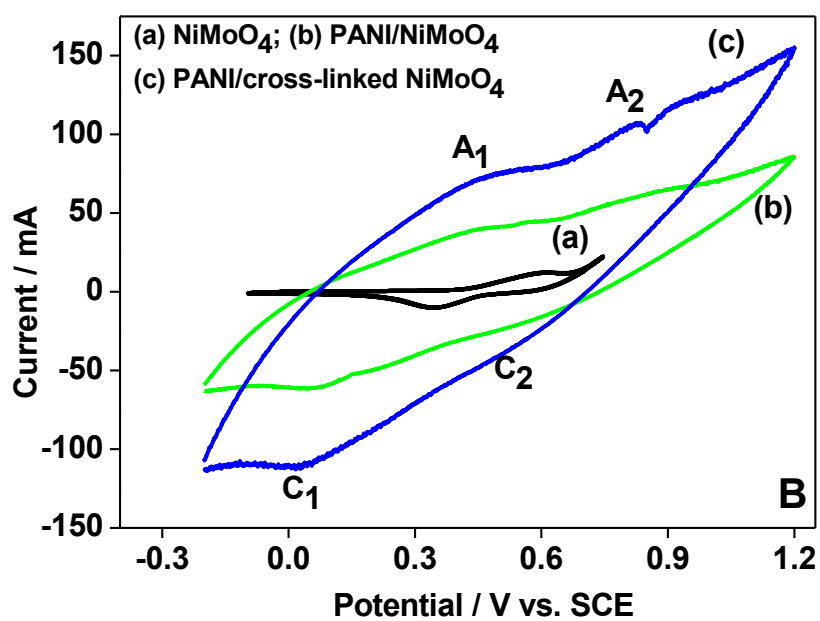
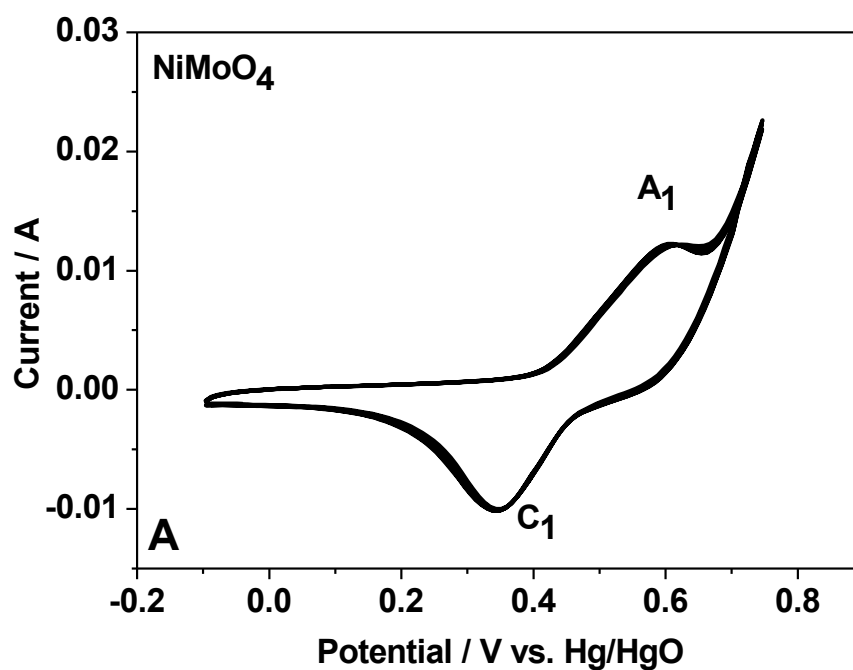


Figure S7 Cyclic voltammogram (a) of as-prepared NiMoO₄ powder and (b) compared the as-prepared NiMoO₄ with the PANI composites under identical conditions.

References

1. P. R. Jothi, K. Shanthi, R. R. Salunkhe, M. Pramanik, V. Malgras, S. M. Alshehri and Y. Yamauchi, *Eur. J. Inorganic Chem.* 2015, **22**, 3694 – 3699.
2. W. Xiao, J. S. Chen, C. M. Li, R. Xu and X. W. Lou. *Chem. Mater.* 2010, **22**, 746 – 754.
3. Y. Ding, Y. Wan, Y.-L. Min, W. Zhang and S.-H. Yu, *Inorganic Chem.* 2008, **47**, 7813 – 7823.
4. N. T. McDevitt and W. L. Baun, *Spectrochim. Acta* 1964, **20**, 799 – 808.
5. P. P. Cod, P. C. G. Panneter and J. Gullermet, *Spectrochim. Acta* 1972, **28**, 1601 – 1613.
6. K. Eda, Y. Kato, Y. Ohshiro, T. Sugitani and M. S. Whittingham, *J. Solid State Chem.* 2010, **183**, 1334 – 1339.